View metadata, citation and similar papers at core.ac.uk

brought to you by CORE

provided by Texas A&M University

ADVANCED 3D PRINTING TO FABRICATE MICROFLUIDIC DEVICES FOR CANCER AND STEM CELLS CO-CULTURE STUDY IN SPACE

A Thesis

by

JASKIRAT SINGH BATRA

Submitted to the Office of Graduate and Professional Studies of
Texas A&M University
in partial fulfillment of the requirements for the degree of

MASTER OF SCIENCE

Chair of Committee,	Jun Kameoka
Committee Members,	Chin B. Su
	Kamran Entesari
	Kung-Hui Chu
Head of Department,	Miroslav Begovic

December 2015

Major Subject: Electrical Engineering

Copyright 2015 Jaskirat Singh Batra

ABSTRACT

Two different type of microfluidic devices were designed, fabricated and tested to capture the microspheres. The passive device seems to be more reliable because of no possibility of damage, whereas the thin film in active device got ruptured when too much pressure was applied to the valve control layer.

The passive design was able to capture microspheres of different sizes. Majority of microspheres captured were between 150-175 microns. The capture efficiency for this device was slightly lower than expected at 26%. This was found to be due to the long channel length which leads to pressure drop towards the end of the channel. In addition, capturing of microspheres causes high resistance to flow towards the end of channel. To the best of my knowledge, this is a first kind of device to capture microspheres at this size range of 125-215 microns. The proof of concept for capturing large particle size >100um and broad size distribution has been demonstrated. The device will be further improved by optimizing the dimensions.

DEDICATION

To my parents, my sister and my family

ACKNOWLEDGEMENTS

I am greatly thankful to all the individuals who have inspired me and encouraged me to carry out this research.

I would like to express my deepest gratitude to my advisor, Dr. Jun Kameoka, for his outstanding guidance, patience and support throughout the course of my research. I would like to give credit to Dr. Kameoka for getting me interested in the area of Micro and Nano-technology through his courses—Nanobiotechnology, Nanotechnology Fabrication and Micro Robotics. I am also thankful to Dr. Kameoka for trusting me and offering unique opportunities to help him write grants, and teach some of the lectures in his course.

I am thankful to all the committee members for their valuable insights and suggestions on my research. I would like to thank Dr. Chin Su for sharing his knowledge and experience related to optical imaging for my research, Dr. Kamran Entesari for collaborating with me on research projects related to microfluidics and liquid metals, and Dr. Kung-Hui Chu for providing me training and access to her lab.

This work is performed in collaboration with Dr. Carl Gregory in Cellular and Molecular Medicine at the Institute for Regenerative Medicine-Texas A&M Health Science Center, and Dr. Roland Kaunas in Biomedical Engineering at Texas A&M University. I am very grateful for their help and support as well. Thanks to Dr. Kaunas for granting me access to his research lab, and Dr. Gregory for providing biological samples

for research. Thanks to the Center for the Advancement of Science in Space (CASIS) for financially supporting this project.

Thanks also go to my friends and colleagues and the department faculty and staff for making my time at Texas A&M University a great experience. I would like to extend my appreciation to graduate students Po-Jung Huang and Lakruwan Samarasinghe for training me for benchwork in our lab, and answering my questions with utmost patience. Thanks to my good friend, Sundeep Sharma, who was always willing to help and give best suggestions. I also want to extend my gratitude to the staff at Materials Characterization Facility and Aggie Fab at Texas A&M University.

Finally, a special thanks to my mother, father and sister for their support and encouragement. I am truly thankful to my parents for always inspiring me and instilling in me a passion for research and discovery. My family is my support system and is always there for me when I need them.

NOMENCLATURE

OEhMSC	Osteogenically Enhanced Human MSCs
MSC	Mesenchymal Stem Cells
SLA	Stereolithography
PDMS	Polydimethylsiloxane
GFP	Green Fluorescent Protein

TABLE OF CONTENTS

Page

LIST OF FIGURES

1. INTRODUCTION

Microfluidics has impacted many different areas of research in the last few years. It has found applications in healthcare diagnostics, biofuel discovery, pharmaceutical research, environmental testing, bio-sensing, etc. Some of the reasons why microfluidic devices have become popular are due to their low-cost, small size (equivalent to a credit card), high-throughput, short turnaround time, and consumption of very small amount of reagents/sample. In some cases, the chemical or biological samples can be recovered after testing. Moreover, these devices can also be automated [1].

Despite all these advantages, the use of microfluidic devices for space applications has not been fully explored. Microfluidic devices, also commonly known as Lab-on-a-chip, can integrate and scale down a complex room-sized laboratory onto a tiny chip. Lower payload requirements for a microfluidic device makes them an ideal platform for space-based science experiments and research [2].

Recently, the first 3D printer in space was launched by National Aeronautics and Space Administration (NASA), and the printer's ability to manufacture parts on demand in space was demonstrated. Additionally, the 3D printers on Earth have already been printing at feature resolution of tens of microns for a while [3-4]. More recently, the 3D printers have been used to make microfluidic devices by replacing silicon-based molds with photo-curable materials in soft lithography process [5-7]. In some cases, 3D printed parts have been used to directly make microfluidic devices, especially where the transparency is not a big concern. As 3D printing evolves into space, it may be possible to

directly print microfluidic devices on-demand. Meanwhile, microfluidic devices can be fabricated on Earth and carried to space for experiments on International Space Station (ISS) and during deep space missions.

As an example, micro-gravity environment in space is suited for 3-dimensional cell cultures which can mimic the physiological micro-environment inside human body [8-9]. Under the influence of gravity, cells settle to the bottom of culture plate and grow only in two dimensions. This prevents the 3-dimensional interactions from taking place between the cells. It has been shown that 3-dimensional interactions are important for cells to form network. By co-culturing cancer cells and human stem cells in space, biologists can establish physiologically relevant 3-dimensional models for cancer metastasis to stem cells (or bone). The 3-dimensional models can provide very powerful platform for studying cancer-stem cell interactions and understanding mechanism involved in metastasis. In other words, micro-gravity environment may establish *in-vitro* models for cancer metastasis on to stem cells [10]. In order to examine a large number of biological samples obtained from co-culture study, the strength of microfluidics can be harnessed [11].

It is of significant interest to study stem (bone) cells and cancer (tumor) interaction because approximately half of the 700,000 newly diagnosed cancers per year in the US will eventually involve bone [12]. The tumor may either initiate within the bone or metastasize to it. Either way, they are likely to disrupt the bone tissue repair, leading to formation of Osteolytic Lesions (OL) or holes in the bone which causes fractures, pain and tumor propagation [13]. In general, bone cancer can be very painful and studying the

tumor-bone interaction can provide answers to bone tissue repair. By conducting experiments in low-gravity, the 3-dimensional interactions can occur between bone-derived stem cells and cancer cells, which can then be studied in a microfluidic device.

The design and fabrication of microfluidic devices to study cancer-stem cell interaction forms an important part of better understanding cancer metastasis. Two such designs were fabricated and tested in this project as a proof of concept. The work presented in this thesis will also demonstrate the application of advanced 3D printing for micro-fabrication of microfluidic devices.

2. BACKGROUND

2.1 Overview of cell/tissue culture methods and effect of low-gravity

There are three main ways of growing cells and tissues, each having their own benefits and limitations.

The most conventional way of growing cells is the *monolayer growth* method in which cells are grown in petri dishes or culture flasks. This is a relatively simple and cheap way of growing large number of cells. The cells settle to bottom of the substrate and growth occurs only in 2-dimensions. This method prevents 3-dimensional interactions from taking place between the cells, and the cells cannot form 3-dimensional networks. The 3-dimensional networks have been shown to be important in mimicking the physiological micro-environment inside the human body [14].

The second method involves the use of *animal models* in which the cells are first grown in-vitro, and then surgically implanted inside the animal. The implanted cells/tissue can then interact with the native animal tissue. This method allows some 3-dimensional interactions between the implanted tissue and host animal. The disadvantage is that this method is relatively more expensive, and the tissue sample has to be removed in order to analyze it [15].

Low-gravity method has been shown to be highly useful in promoting the three-dimensional interactions between the cells. In the absence of gravity, cells cannot settle to the bottom of the substrate. Instead, cells can communicate with each other and form three-dimensional aggregates that can be easily studied. The main challenge in using this method

is that it requires low-gravity, but it can also provide physiologically useful cell/tissue models [8-9,10].

2.2 Microspheres as scaffolds for cell growth

Microspheres have been readily used as cell carriers in many culture experiments because of the cell's ability to attach to them. In many cases, collagen microspheres have been used because of their relevance to extracellular matrix present in the body [16]. Collagen is a protein present in connective tissue that holds the cells together, and collagen microspheres can provide initial micro-environment for cells to attach. In this project, Cytodex-3 (GE Healthcare Life Sciences) microspheres were used because they can be easily prepared by swelling them in PBS for 3 hours. Figure 1 shows schematic of microsphere with inner layer made from cross-linked dextran and the outer surface coated with collagen. The manufacturer's specifications mention the average particle size to be 175μm after swelling, but it was found to be 125-225μm.

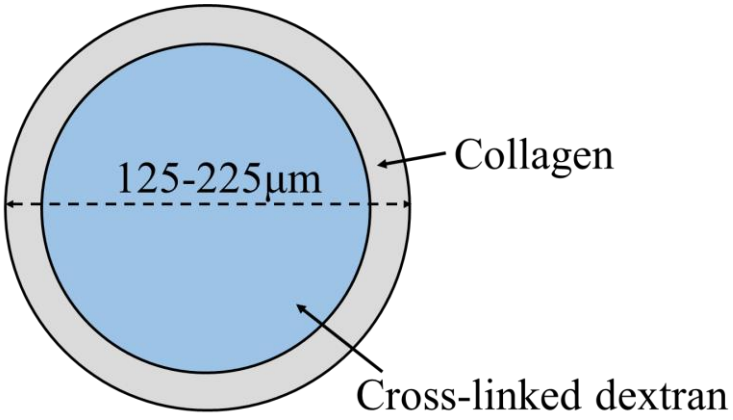

Figure 1: Schematic diagram for structure of Cytodex-3 (GE) microsphere [17].

2.3 Rotating Wall Vessel (RWV) for three-dimensional culture

On Earth, the micro-gravity effects during cell culture can be simulated using a low-gravity bioreactor, called RWV. This vessel consists of chambers which are filled with cell-laden microspheres and the growth media for cells, as shown in Figure 2 (left). The rotation of vessel causes the microspheres to move close to center, where the cells on microspheres can interact with each other (Figure 2-right). It is important to note that even though the cells are attached to microspheres, they can readily interact with cells from other microspheres, leading to a pseudo-three dimensional interaction between the cells of different microspheres. The purpose of RWV in this project is to simulate low-gravity on Earth in order to develop the co-culture models, and test the microfluidic device before sending to space.

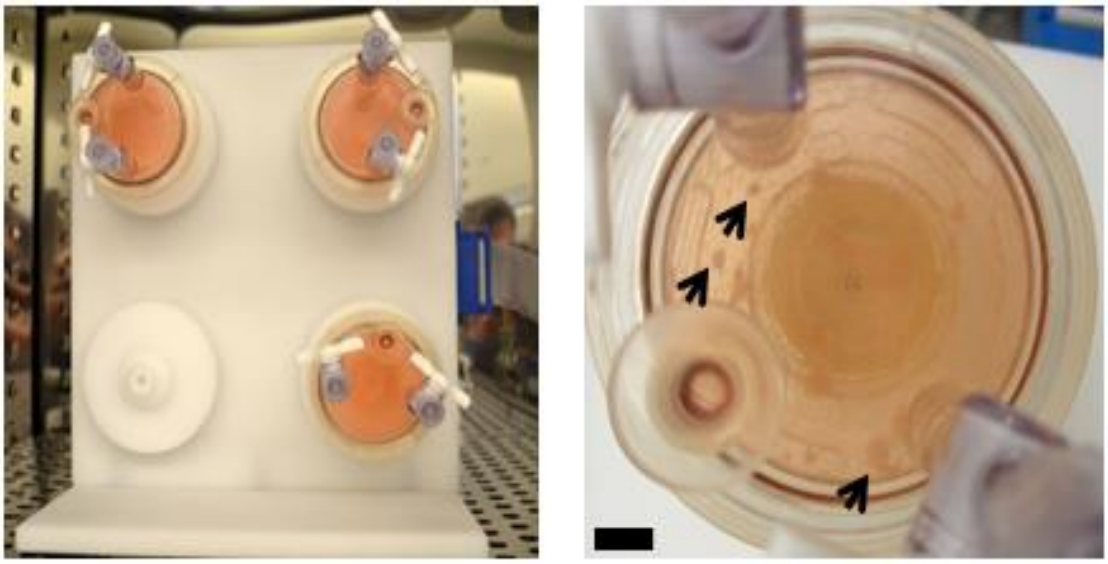

Figure 2: Photo of a rotating wall vessel (RWV). RWV set up showing 3 15mL cultures (left), and aggregates of cell-laden microspheres (right). Reprinted with permission from [18].

2.4 Cancer-stem cell interaction and co-cultures

It is known that bone tumors secrete factors to degrade bone tissues, and inhibit bone repair. While the drugs exist today to delay bone degradation, but they lack ability to promote repairing of already degraded bone OLs [18-23]. By co-culturing cancer MOSJ and OEhMSCs (stem cells) on osteogenic microspheres within RWV, it may be possible to replicate the same interactions as those between bone tumor and regenerating bone tissue.

For co-culture samples prepared in Dr. Greogry's lab [18], OEhMSCs and MOSJ-Dkk1 cells are loaded on separate microspheres, and co-cultured in a RWV to allow the interactions between cells to take place. This is shown in Figure 3A. The OEhMSCs are tagged with GFP, and MOSJ-Dkk1 are tagged with red protein to study interactions between the different kinds of cells on microspheres. Under normal gravity, the cells, or the microspheres containing cells would just settle to the bottom of the substrate (Figure 3B).

Figure 4 shows the example of fluorescent images of the co-culture samples of OEhMSCs and MOSJ-Dkk1 obtained from analyzing them. These images were not taken in a microfluidic device.

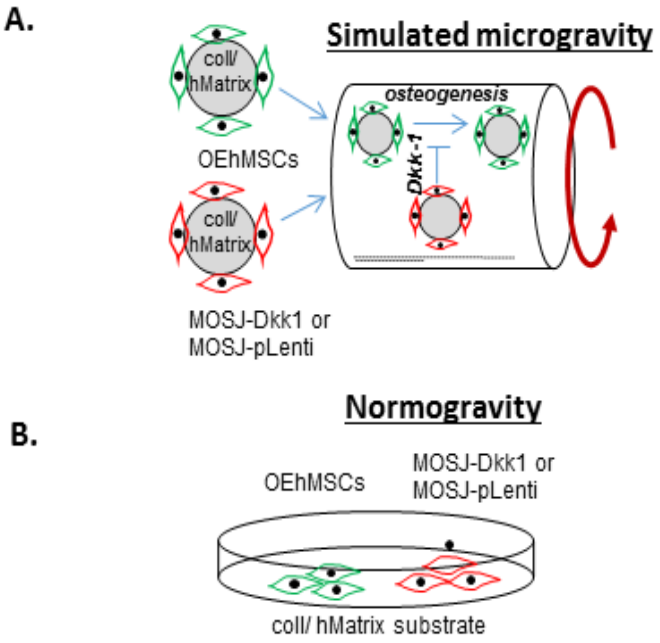

Figure 3: Schematic of cell co-culture. (a) OEhMSCs containing green fluorescent tag, and MOSJ-Dkk1 containing red fluorescent tag co-cultured in a RWV to simulate microgravity, (b) OEhMSCs and MOSJ-Dkk1 settle to bottom of the cells under normal gravity. Reprinted with permission from [18].

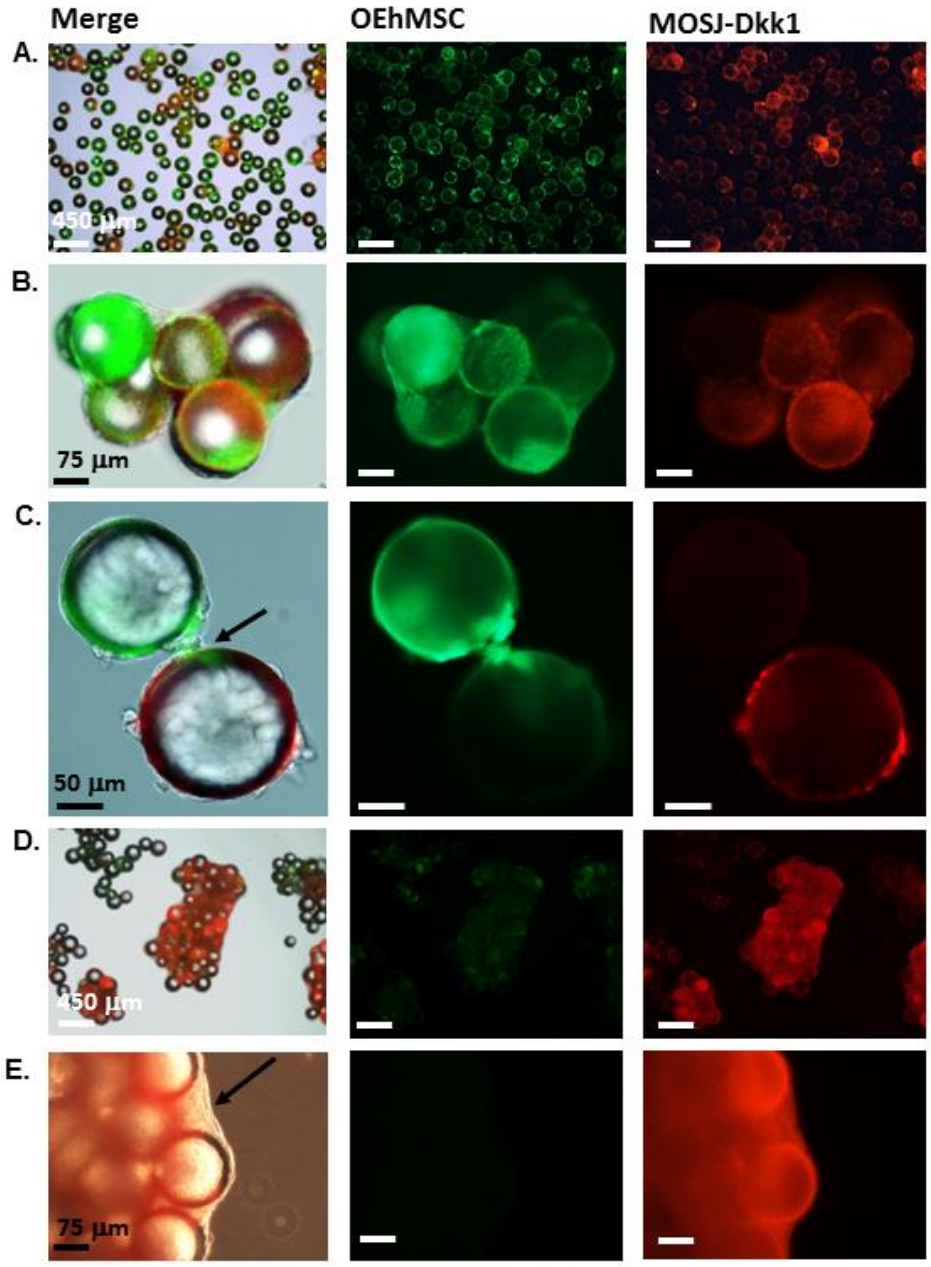

Figure 4: Fluorescent images showing co-culture samples of OEhMSCs and MOSJ-Dkk1 cells from RWV on collagen coated beads (a-c) and hMatrix coated beads (d-e). OEhMSCs emitting green signal (middle), MOSJ-Dkk1 emitting red signal (right), and merge of two signals (left). Note: Images were taken without microfluidic device. Reprinted with permission from [18].

2.5 Microfluidic technology and particle trapping

Microfluidic devices have previously been used for particle (cells, beads, spheres, etc.) trapping. Various trapping methods including the optical, chemical, hydrodynamic, magnetic, electric, and acoustic capturing methods have been demonstrated in microfluidic devices [24-25]. The external electric, magnetic or chemical fields in a cell experiment can affect the cell physiology. The optical methods that require high power can produce heat, and also affect the cell. On the other hand, hydrodynamic trapping is usually based on mechanical 'obstacles' or 'barriers' [24]. Hence, hydrodynamic trapping is a relatively simple, inexpensive and preferred method to implement large-scale trapping of biologically relevant particles (containing cells) in a microfluidic device.

Many hydrodynamic particle trapping devices have been reported by other researchers that can trap small single-particles close to 10μm in cells. Surprisingly, there are not many devices that have been designed to trap single particles of larger dimensions >100μm. Table 1 shows a summary of research conducted on trapping particles of different sizes, the type of particle (living cells vs. non-living beads/microspheres), and the capture efficiency. The trapping of small particles is relatively easier in a hydrodynamic trapping device compared to large particles. This could be due to several reasons, including the fact that larger particles are more difficult to stop with an obstacle compared to small ones. Tan et. al. reported that they were able to capture 15μm single cells with a 99% capture rate, while they had difficulty when working with 99μm polystyrene beads in >100μm channels [27, 37]. Consequently, the capture rate for large particle trapping was not reported.

Table 1: Summary of capture efficiency for different particles in microfluidic devices

Particle size (μm)	Particle type	Single particle Capture rate/efficiency	Reference
17±1.5	cells	89 %	26
15±0.3	cells	99 %	27
15	cells	55 %	28
0.5-2	bacteria (rod)	60 %	29
13	cells	10-20 %	30
15, 6, 4	microspheres	70, 40, 30 %	31
10	microspheres	99 %	32
5, 7.7	microspheres	96, 91 %	33
7.5	microspheres	99 %	34
10	cells	81 %	35
20±3	cells	62 %	36
98.7±1.0	beads	Not reported	37

For small particle trapping, Di Carlo et. al. designed obstacles or barriers to capture 15μm cells flowing in a liquid with 55% capture rate for single cells [28]. These barriers acted as trap sites for individual cells and a large density were packed on a single device. In some cases, the barriers also prevented cells from moving into the trap sites, hence the trapping efficiency was relatively low. An improvement to previous closed-trap design was suggested by Wlodkowic et. al. in which they made small gaps in barriers to allow fluid to flow through the trap region, and encourage cells to move into the trap sites [30]. Even with the fluid flowing through the trap region, the capture efficiency was reported to be 10-20% and majority of the cells could not be individually captured in the trap sites.

Previous designs were further refined by Tan and Takeuchi by controlling the fluidic resistance to perform hydrodynamic cell trapping [27, 37]. By manipulating the

channel dimensions, they could control the fluidic resistance along a channel, which in turn was used to move micro-particles along different paths in to the trap sites. When the trap site was unoccupied, the low fluidic resistance allowed micro-particles (cells or beads) to move in to the trap site. Once the particle was trapped, the fluidic resistance along the captured path increased, and the rest of the particles had to move around the trap site to a lower fluidic resistance path. They were able to successfully capture 15μm cells with very high capture rate, however they faced problems when using 99μm beads in the same design. Despite having high capture efficiency for small particles, their design was limited to trapping particles of a specific size. This further limits the use of their device in a realistic application where the sizes of particles may vary.

Similarly, Xu et. al. improved the obstacles with gaps design reported earlier by optimizing the dimensions of the obstacles and gaps relative to particle size [32-34]. They compared their optimized design to un-optimized, and reported very high capturing efficiency of >90% for microsphere sizes between 5 to 10μm. Even then, their designs were made for specific particle size with a very narrow size distribution, which again limits the usability in a real-world application with varying particle sizes.

To overcome the limitations of previous designs, Kim. et. al. designed a device with different zones for trapping particles of three different sizes (4, 6 and 15μm) [31]. Bigger particles were captured in the first zone, allowing smaller particles to flow through. Smaller particles were captured further down in the next two zones. This device captured single particles with 70% trapping efficiency in the first zone, which decreased rapidly to

40% and 30% in the next two zones. Sorting of particles is achieved by this device in particles with narrow size distributions.

A plot showing capture efficiency for trapping particles of various sizes is shown in Figure 5. This plot is generated from references to previous literature with their reported capture efficiency, and it shows that previous works have focused mainly on capturing small particles (0.5-20μm). Xu et. al. tested their design with beads (~100μm) and reported having difficulty at large particle dimension [37]. My goal in this project is to test and extend the capturing capability of microfluidic device for large particle dimensions between 125 to 230μm. In other words, my aim is to push the particle capturing capability of microfluidics to the right-hand side of plot shown in Figure 6. The eventual plan is to focus on target region shown in Figure 6.

Figure 5: A plot of capture rate/efficiency for different sizes of single particles trapped previously in literature. The reference to each data point is provided next to it. The inset plot is data magnified to small particle region. No existing data point for large particle region (>100um) could be found. The blue box shows the ideal target region for device.

3. MICROFLUIDIC DEVICE DESIGN

The goal of this project is to design a microfluidic-based platform for the characterization of cell-cell interaction based on cellular fluorescence signals of Osteochondral sarcoma line MOSJ and Osteogenically Enhanced Human Mesenchymal Stem Cells (OEhMSC) on collagen-coated microspheres.

In this thesis, the device is utilized to capture collagen-coated microspheres without cells attached to microsphere surface. This is mainly to demonstrate the capability of microfluidic device to capture 125-215 microns microspheres as a proof of concept. In this section, the rationale and factors to take into account during design are presented, followed by two different designs of microfluidic device.

The main factors to take into account when designing a microfluidic device for microsphere capturing and fluorescent imaging are:

(a) Large variation in size of the microsphere particles makes it difficult to capture them all with uniform dimensions of trap.

(b) Larger particles contain more energy compared to small particles.

(c) The microspheres should have minimum contact with the walls of the channel for imaging purposes.

The basic rationale when designing a chip was to have the ability to capture the microspheres and once the microspheres are in the device, they should be held stationary within the field of view of the microscope. The chip should be optically transparent so that

the fluorescent signal from cells on microspheres can be measured. Two different designs of microfluidic chip were made based on the capturing mechanism.

3.1 Active design

The active design contains active pneumatic valves to capture individual microspheres at specific locations inside the chip. Microfluidic device is made of three layers of PDMS—top layer with channels for microspheres to flow, a thin middle active pneumatic layer, and the bottom layer with channels for air to flow. The actual photo image of microfluidic chip is shown in Figure 6a. As air pressure is applied into the bottom layer through the air channel, the middle layer deforms to partially close the top layer channels. The array patterns of sample and valve channels should trap multiple collagen microspheres (Figure 6b). By trapping multiple microspheres away from each other and exposing them to an excitation wavelength of light, the signals could be recorded from multiple microspheres at once allowing for a high throughput of the device.

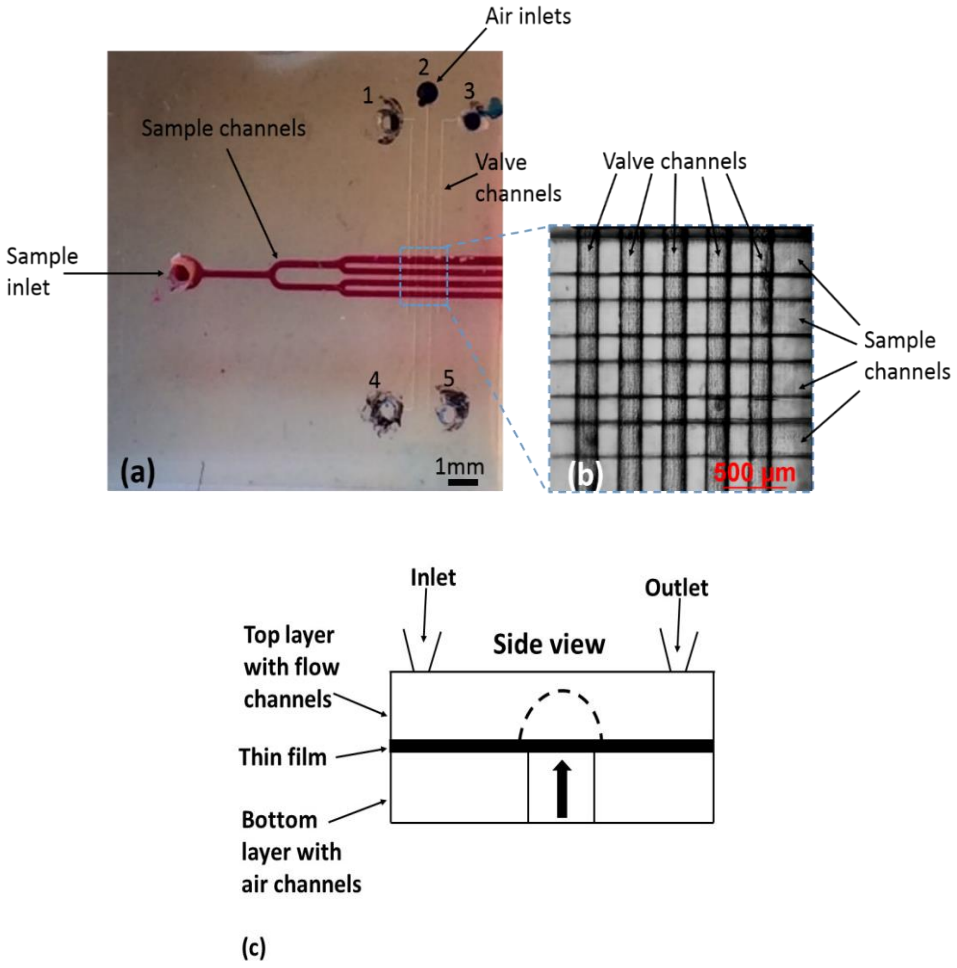

Figure 6: Concept of active microfluidic device. (a) Image of microfluidic device (top view) showing the microfluidic channels (width 200um) for sample which are colored red for illustration. Normal to sample channels are the valve channels with inlets for air shown using 1-5, (b) Magnified image of microfluidic device showing sample and valve microchannels normal to each other, (c) Side view of the channel showing three layers and the middle layer deformation due to pneumatic actuation.

The active device allows high throughput of microspheres to be flown but the pneumatic valves made out of polydimethylsiloxane (PDMS) were found to get damaged over time. Because of the energy of microspheres flowing in the channel, the thin

pneumatic valves could not capture the microspheres and would rupture (shown in Figure 7).

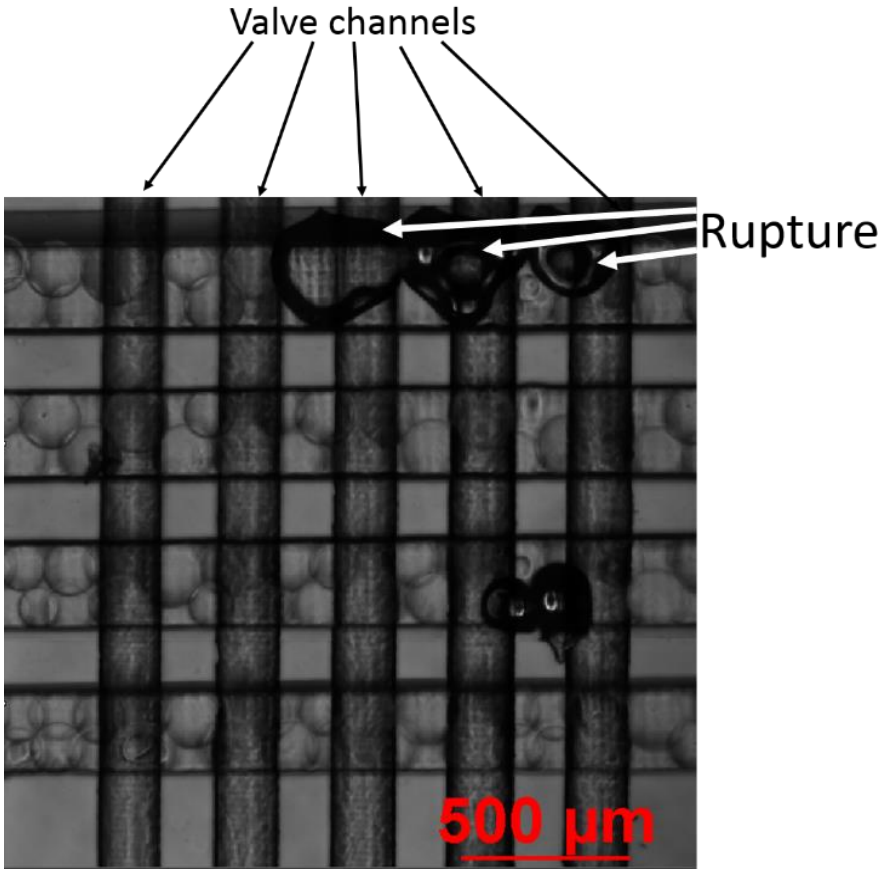

Figure 7: Microscopic view of active device showing microspheres flowing through the liquid flow channels. Rupturing of pneumatic film is also shown on the right hand side.

3.2 Passive design

The passive design contains ‘obstacles’ or trap sites to allow the microspheres to get stuck in the wells as they are flowing through the channel. The unique feature of this chip is that the trap sites are three-dimensional which have not been developed before.

Microfluidic device is made of two layers—top PDMS layer for inlets/outlets, and bottom PDMS layer with channels and passive traps for microspheres. The actual photo image of microfluidic chip is shown in Figure 8, and the schematic of trap design is shown in Figure 9.

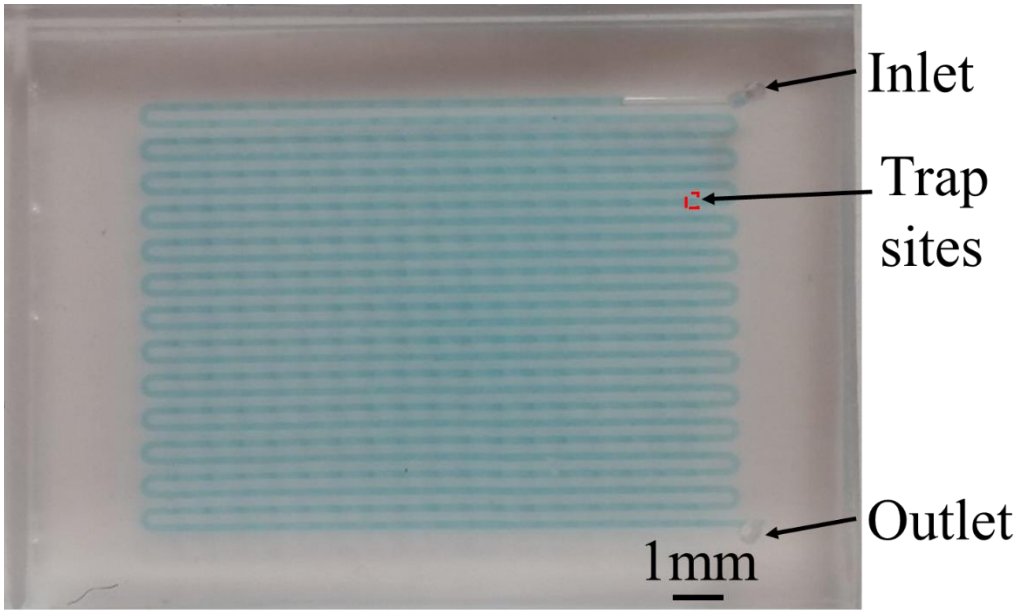

Figure 8: Photo of passive microfluidic device showing inlet and outlet. The channels are filled with blue dye to show the channels. A single trap site is shown with a red box.

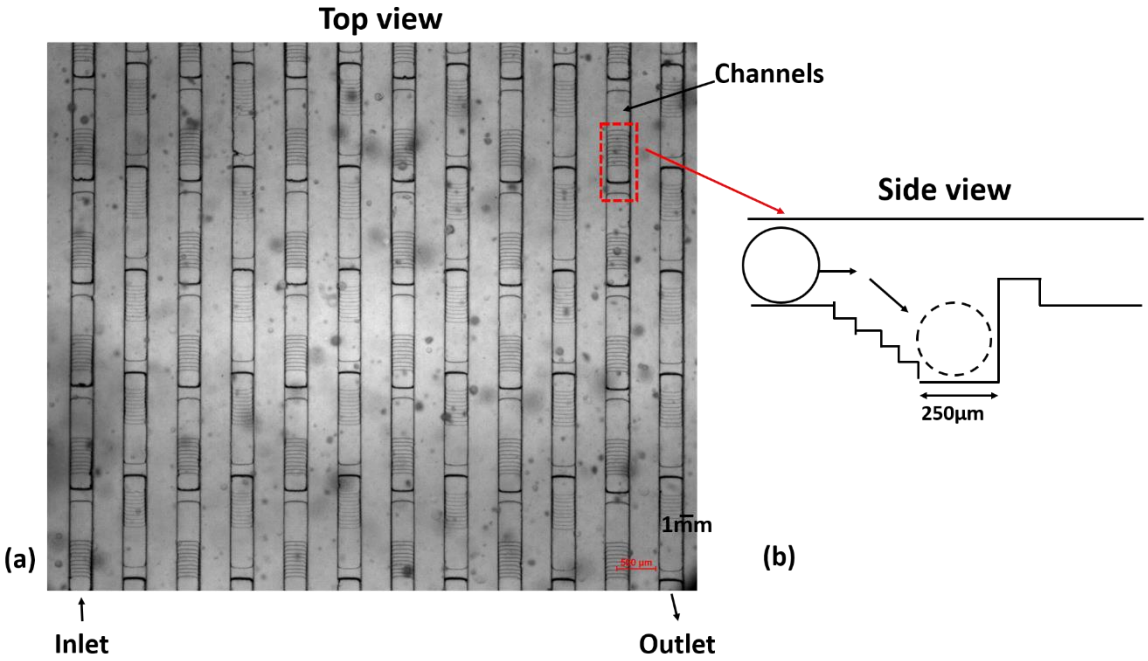

Figure 9: Concept of passive microfluidic device. (a) Microscopic image of microfluidic device (top view) showing the microfluidic channels (width 200um) which are designed parallel to each other, and (b) Schematic diagram showing side view of microsphere trap. The microspheres flow down the slope and get trapped in wells.

The microspheres are introduced in microfluidic device using inlet, and once microspheres are flown through the channel, they encounter the slope which traps them at the bottom of the channel. Rest of the microspheres can continue to flow through the channel until they encounter other traps. Once the microspheres are trapped, they can be excited using fluorescent signal, and the emitted red/green signals can be recorded. The stair-step pattern of slope is caused due to resolution of 3D printer, but the size of step is very small compared to the size of microspheres (125-215 µm).

4. MICROFLUIDIC CHANNEL FABRICATION

4.1 Advanced 3D printing

Many different 3D printers have been used in last few years to fabricate molds for microfluidic devices. Even though there are several different options of 3D printers available—Extrusion, Stereolithography and Poly Jet—the stereolithography printer delivered the best resolution. First, the Computer Aided Design (CAD) of a 3D mold is drawn in SolidWorks software. The 3D model is converted to an STL file which is accepted by the 3D printer software. Envision Tec Micro 3D printer was used with resolution of 30um in X, Y and 25um in Z direction. This printer uses three softwares. The first software inputs the STL file format and checks for errors, dimensions, sets up the file on platform, and makes sure that printer can print the design. In addition, the same software also generates/exports support structure to allow the model to be printed upside-down on a rising platform in stereolithography printer. The second software imports the design file and the support file, and combines them on the print platform. This generates masks/images and the settings that are used to project UV pattern on the printer tray. The third software imports the masks and the settings to handle each print job. It acts as the interface between the printer hardware and the design file. Figure 10 shows the work flow of mold making and PDMS device fabrication.

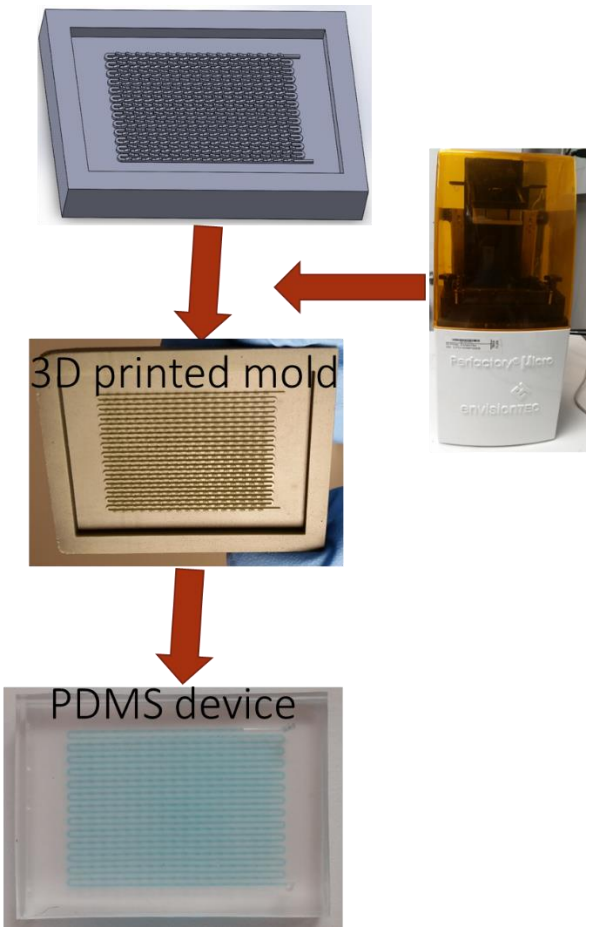

Figure 10: Work flow of mold making and PDMS device fabrication.

4.2 Fabrication of microfluidic channel

The microfluidic device is fabricated in two layers, as shown in Figure 11. A 3D printed mold is obtained using high-resolution printer, as mentioned in section 4.1. The mold is cleaned with isopropyl alcohol (IPA) and dried in oven at 65°C overnight (Step 1). PDMS solution is prepared by mixing Sylgard 184 resin and cure in 10:1 ratio and degassing. The solution is poured in mold and left in oven for 2 hours at 65°C (Step 2). The cured PDMS containing channels is removed from the mold. Another flat piece of

PDMS is prepared and inlet/outlet holes are made using a lab hole puncture (Step 3). The PDMS top and bottom layers are bonded to each other by exposing to oxygen plasma for 1 minute (Step 4). The tubing is inserted in inlet and outlet holes to flow the liquid through the microfluidic device (Step 5).

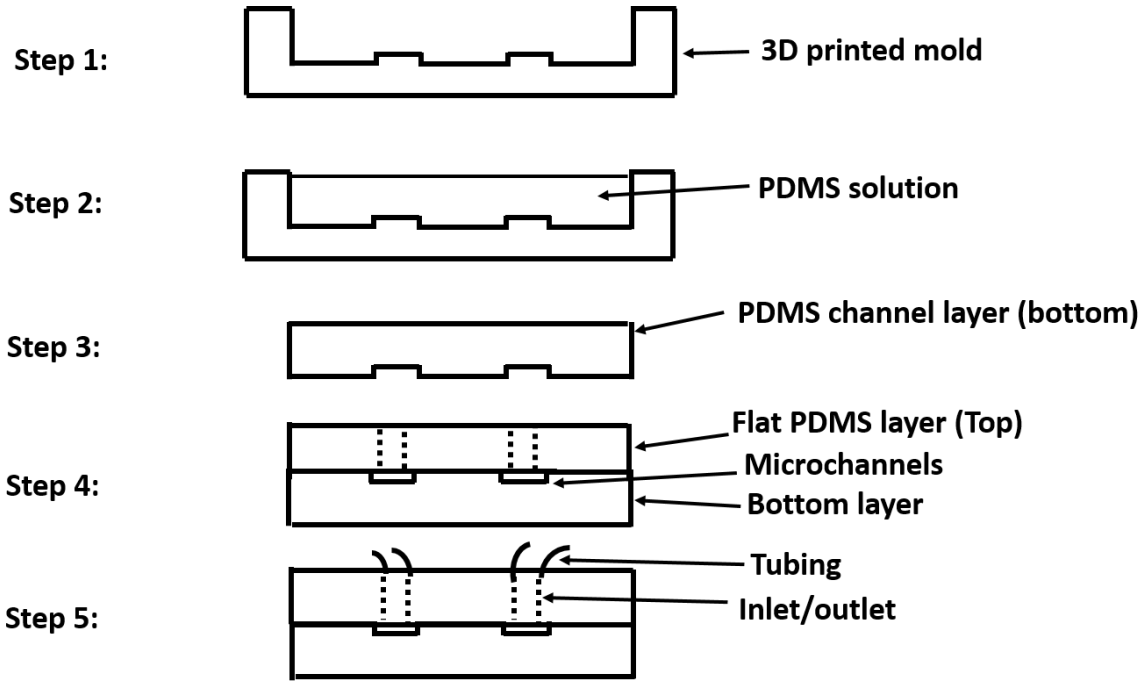

Figure 11: Step-by-step fabrication process (side view) for fabrication of passive microfluidic device.

4.3 Surface modification of microfluidic device

The outer layer of collagen on microspheres sticks to hydrophobic PDMS. Also the cells covered on collagen can adhere to PDMS surface. To avoid this issue, several

surface treatments were tried. The one that worked best was to use small amount of Pluronic 127 mixed with ethanol in PDMS. Pluronic 127 has a PEO-PPO-PEO structure in which the PEO chain move to the surface when channel is exposed to water or PBS. This prevents collagen from sticking to the PDMS surface.

5. METHODS FOR MICROSPHERE TRAPPING AND FLUORESCENCE DETECTION IN FLUIDIC CHANNEL

5.1 Experiment setup

The schematic of experiment and the actual setup is shown in Figure 12 (a, b). Microfluidic device is placed on fluorescent detection platform. The detection platform is connected to fluorescence light source and the filters that can control the excitation and radiation wavelengths. The filters and light sources are automatically controlled by motor connected to the NIS software. Microfluidic device is connected to syringe through an inlet. The syringe contains the microsphere and the samples to be injected. The flow rate of syringe can be controlled by using a syringe pump. The outlet of the microfluidic device is connected to a collection chamber for waste.

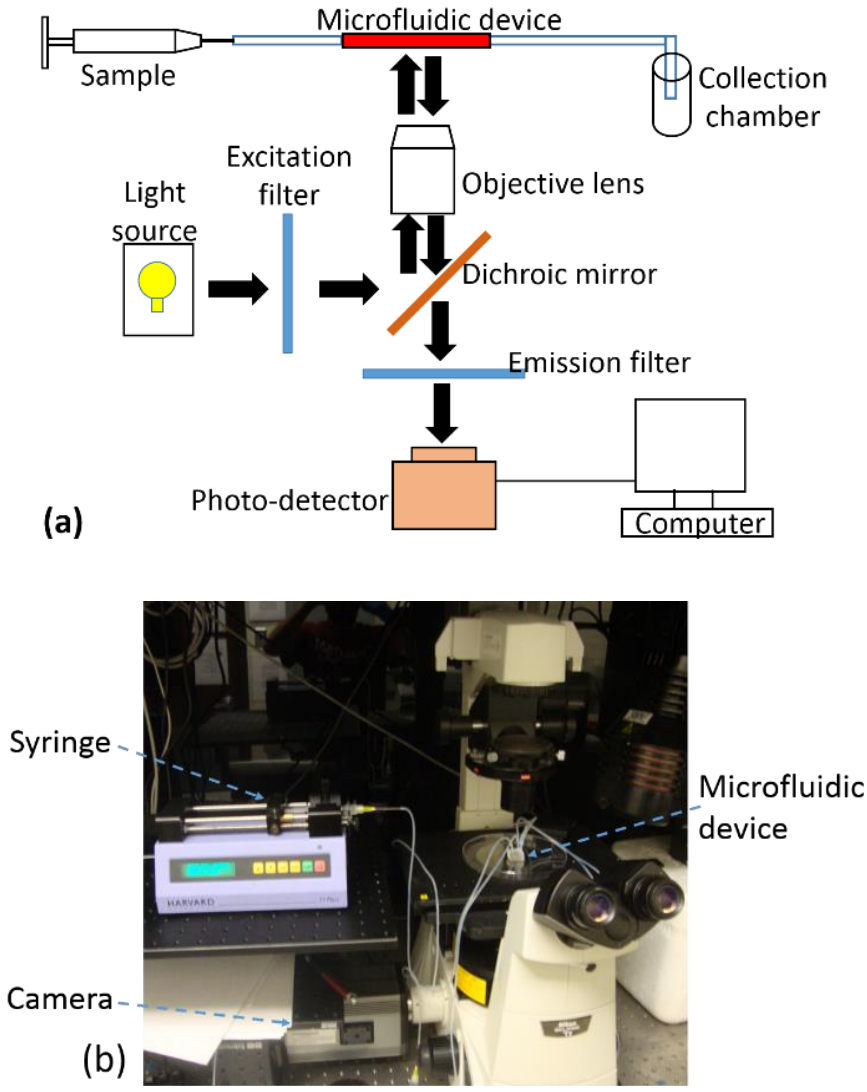

Figure 12: Setup of detection platform. (a) Schematic diagram of optical detection platform with microfluidic device, and (b) Photo Image showing the syringe, pump, microfluidic chip on a platform, camera and the microscope.

5.2 Experiment procedure

The syringe is filled with microsphere solution to be tested and connected to microfluidic device using Tygon tubing. First a buffer (PBS) is flown through the microfluidic device to cause wetting of the channels and allow PEO chains in Pluronic 127 to move to the surface. One the walls of the channel look completely immersed in buffer, the solution containing microsphere is injected into the microfluidic device. For characterization and optimizing the device, Cytodex-3 (GE) microspheres coated with collagen were used.

5.2.1 Active device

Initial results showed that the collagen microspheres can flow through multiple sample channels when they are mixed with PBS and surfactant. Collagen microspheres tend to adhere to PDMS surface since hydrophobic proteins establish hydrophobic interaction with PDMS surface if it is untreated.

Multiple Cytodex-3 collagen microspheres are shown inside the sample microchannels as shown in Figure 13. Multiple collagen microspheres are trapped between active pneumatic valves. This is because the Cytodex-3 microspheres were approximately 150μm in diameter, which is much smaller than the channel width. When the microspheres were injected into the active device and the pneumatic valves were actuated, the valves pushed against the channel to trap the microspheres. In some cases, microspheres were trapped but due to the size of microspheres and lot of inertia in them, microspheres could cause rupturing of pneumatic valve thin film. This is shown in Figure 14.

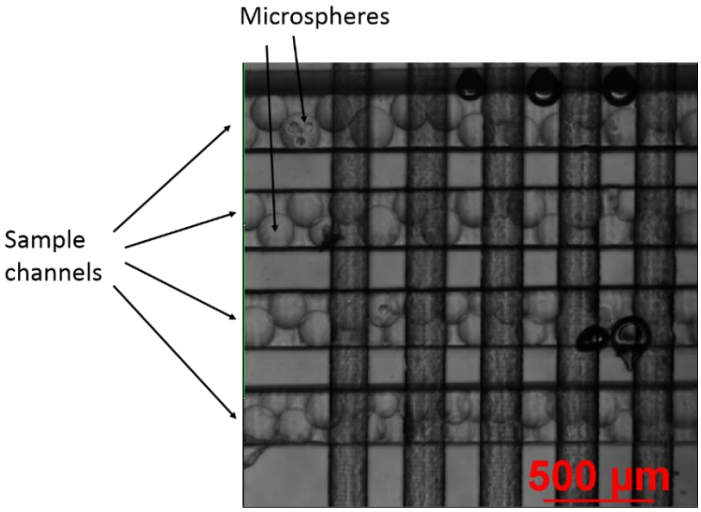

Figure 13: Image showing Cytodex-3 microspheres contained inside the sample channels. Each sample channel has 200 um width.

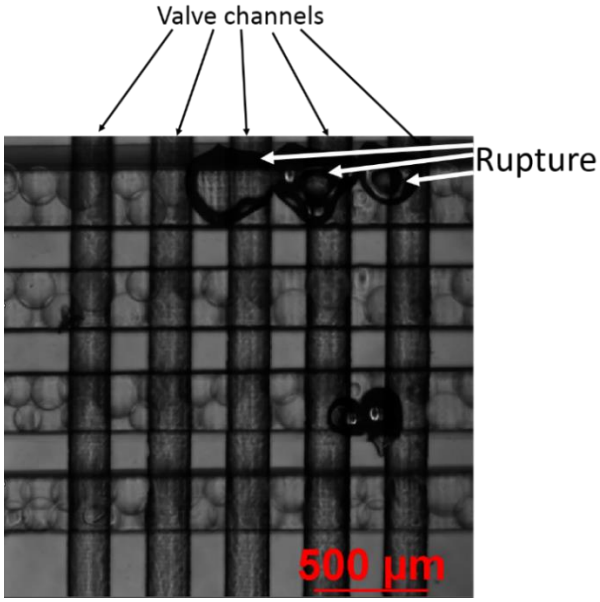

Figure 14: Microscopic image showing valves of active microfluidic device getting damaged as the middle film of PDMS ruptures.

5.2.2 Passive device

The Cytodex-3 (GE) microspheres are flown into the inlet using syringe pump. As microspheres are flown through the channel, they are trapped in multiple traps inside the microfluidic device. Once trapped, microspheres stay in each trap while other microspheres could move through the channel. Multiple Cytodex-3 collagen microspheres are shown trapped inside the microchannels as shown in Figure 15.

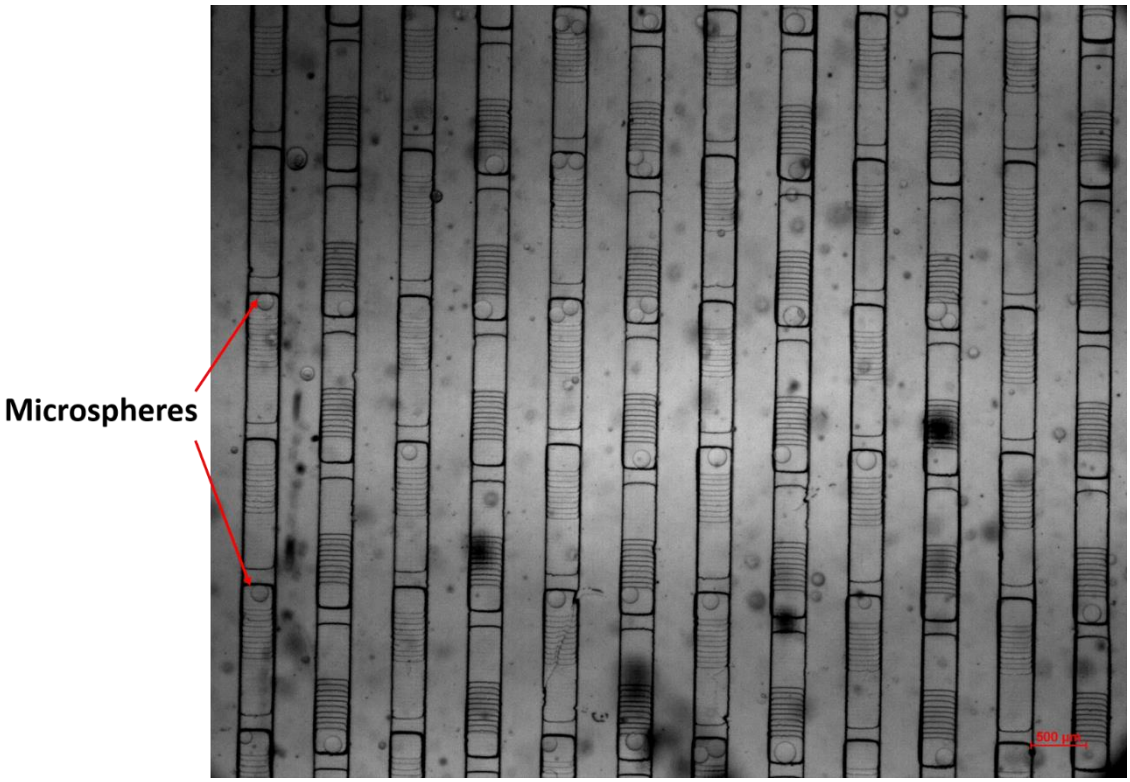

Figure 15: Microscope image showing Cytodex-3 microspheres trapped after the slope in channel of a passive microfluidic device.

6. RESULTS AND DISCUSSION

The microspheres captured in passive device showed a distribution in size given by Figure 16. It shows that majority of the microspheres that were captured were in range of 150 to 175um. Few other size of microspheres were trapped but were mainly removed through the outlet.

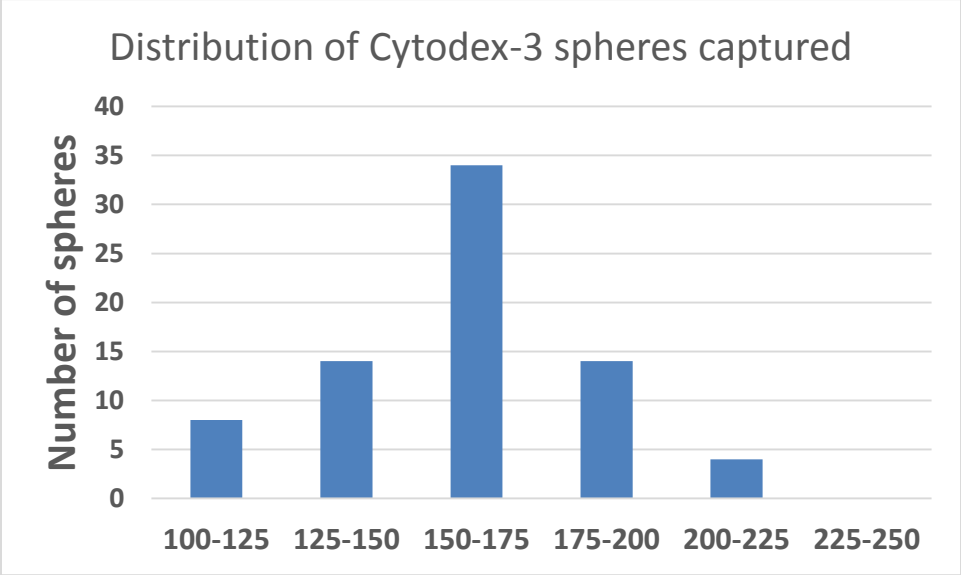

Figure 16: Distribution of single microspheres that are trapped inside the passive microfluidic device.

Initially, single microspheres were observed to be captured in 111 traps out of 425 total traps. The trapping efficiency was calculated to be approximately 26%. This trapping efficiency can be improved by making the sizes of microspheres uniform. The lower trapping efficiency can be explained due to long length of the channel of the device.

Towards the last traps of the channel, fewer microspheres are trapped. This could be due to high resistance to flow that is caused by the microspheres that are captured in the beginning of the channel.

On magnification of device, it was observed that the trapping efficiency was higher closer to the inlet and it dropped further away from the inlet. This further supports the hypothesis that the long channel length could lower the trapping efficiency of microfluidic device.

7. SUMMARY AND CONCLUSIONS

Two different type of microfluidic devices were designed, fabricated and tested to capture the microspheres. The passive device seems to be more reliable because of no possibility of damage, whereas the thin film in active device got ruptured when too much pressure was applied to the valve control layer.

The passive design was able to capture microspheres of different sizes. Majority of microspheres captured were between 150-175 microns. The capture efficiency for this device was slightly lower than expected at 26%. This was found to be due to the long channel length which leads to pressure drop towards the end of the channel. In addition, capturing of microspheres causes high resistance to flow towards the end of channel. To the best of my knowledge, this is a first kind of device to capture microspheres at this size range of 125-215 microns. Previous works which claim to have high capture efficiency, all focus on very small particles from 5-20 microns. This device that can capture microspheres of 125-215 microns will be useful for co-culture sample analysis in space experiments.

Additionally, the application of 3D printing to fabricating microfluidic devices was demonstrated by making molds with smallest feature length of 50 microns. This will be useful for other microfluidic research groups, as well as for future fabrication of microfluidic devices in space.

The proof of concept of trapping of large particle size (>100um), with broad size distribution (125-215um) in a microfluidic device has been demonstrated as proof of concept. The device will be further improved by optimizing the channel dimensions and flow parameters.

Finally, the purpose of RWV in this project is to simulate low-gravity on Earth in order to develop the co-culture models and test the microfluidic device before sending to space. The future goal of this project is to perform micro-gravity studies on International Space Station (ISS) without the need for RWV, and analyzing the co-culture using the microfluidic device demonstrated in this project.

REFERENCES

1. D. Mark, S. Haeberle, G. Roth, F. Stetten and R. Zengerle, "Microfluidic lab-on-a-chip platforms: requirements, characteristics and applications," *Chemical Society Reviews*, 2010, **39**, 1153–1182.
2. N. Leach, "3D Printing in Space," *Architectural Design*, 2014, **84**, 108–113.
3. R. Liska, M. Schuster, R. Infu¨hr, C. Turecek, C. Fritscher, B. Seidl, V. Schmidt, L. Kuna, A. Haase, F. Varga, H. Lichtenegger and J. Stampf, "Photopolymers for rapid prototyping," *Journal of Coatings Technology and Research*, 2007, **4 (4)**, 505–510.
4. Perfactory Micro HiRes, EnvisionTec Inc., Michigan, USA.
5. A. P. Saghati, J. S. Batra, J. Kameoka and K. Entesari, "A microfluidically-reconfigurable dual-band slot antenna with a frequency coverage ratio of 3:1," *IEEE Antennas and Wireless Propagation Letters*, 2015.
6. A. P. Saghati, J. S. Batra, J. Kameoka and K. Entesari, "Miniature and reconfigurable CPW folded slot antennas employing liquid-metal capacitive loading," *IEEE Transactions on Antennas and Propagation*, 2015, **63**, 9, 1.
7. A. P. Saghati, J. S. Batra, J. Kameoka and K. Entesari, "A miniaturized microfluidically reconfigurable coplanar waveguide bandpass filter with maximum power handling of 10 watts," *IEEE Transactions on Microwave Theory and Techniques*, 2015, **63**, 8, 1-11.
8. B.R. Unsworth and P.I. Lelkes, "Growing tissues in microgravity," *Nature Medicine*, 1998, **4**, 8.

9. R. P. Schwarz, T. J. Goodwin and D. A. Wolf, "Cell culture for three- dimensional modeling in rotating-wall vessels: An application of simulated microgravity," *Journal of Tissue Culture Methods*, 1992, **14**, 51-58.
10. J. L. Becker and G. R. Souza, "Using space-based investigations to inform cancer research on Earth," *Nature Reviews Cancer*, 2013, **13**, 315-327.
11. Y. Huang, B. Agrawal, D. Sun, J. S. Kuo and J. C. Williams, "Microfluidics-based devices: New tools for studying cancer and cancer stem cell migration," *Biomicrofluidics*, 2011, **5**, 013412.
12. G. R. Mundy, "Metastasis to bone: causes, consequences and therapeutic opportunities," *Nat Rev Cancer*, 2002, **2**, 584-593.
13. F. Saad, A. Lipton, R. Cook, Y. M. Chen, M. Smith and R. Coleman, "Pathologic fractures correlate with reduced survival in patients with malignant bone disease," *Cancer*, 2007, **110**, 1860-1867.
14. K. Chitcholtan, E. Asselin, S. Parent, P. H. Sykes and J. J. Evans, "Differences in growth properties of endometrial cancer in three dimensional (3D) culture and 2D cell monolayer," *Experimental Cell Research*, 2013, **319**, 75-87.
15. K. Yamada and E. Cukierman, "Modeling Tissue Morphogenesis and Cancer in 3D," *Cell*, 2007, **130**, 4, 601-610.
16. L. Yao, F. Phan and Y. Li, "Collagen microsphere serving as a cell carrier supports oligodendrocyte progenitor cell growth and differentiation for neurite myelination *in vitro*," *Stem Cell Research & Therapy*, 2013, **4**, 109.
17. GE Healthcare Life Sciences, Cytodex surface microcarriers. Technical data sheet.

18. Dr. Carl Gregory's lab, Institute for Regenerative Medicine-Texas A&M Health Science Center (*Unpublished*).
19. E. Tian, F. Zhan, R. Walker, E. Rasmussen, Y. Ma, B. Barlogie and J. D. Shaughnessy, Jr., "The role of the Wnt-signaling antagonist DKK1 in the development of osteolytic lesions in multiple myeloma," *N Engl J Med*, 2003, **349**, 2483-2494.
20. C. A. Gregory, W. G. Gunn, E. Reyes, A. J. Smolarz, J. Munoz, J. L. Spees and D. J. Prockop, "How Wnt signaling affects bone repair by mesenchymal stem cells from the bone marrow," *Ann N Y Acad Sci*, 2005, **1049**, 97-106.
21. N. Lee, A. J. Smolarz, S. Olson, O. David, J. Reiser, R. Kutner, N. C. Daw, D. J. Prockop, E. M. Horwitz and C. A. Gregory, "A potential role for Dkk-1 in the pathogenesis of osteosarcoma predicts novel diagnostic and treatment strategies," *Br J Cancer*, 2007, **97**, 1552-1559.
22. Y. Cai, A. B. Mohseny, M. Karperien, P. C. Hogendoorn, G. Zhou and A. M. Cleton-Jansen, "Inactive Wnt/beta-catenin pathway in conventional high-grade osteosarcoma," *J Pathol*, 2010**, 220**, 24-33.
23. N. K. Thudi, C. K. Martin, S. Murahari, S. T. Shu, L. G. Lanigan, J. L. Werbeck, E. T. Keller, L. K. McCauley, J. J. Pinzone and T. J. Rosol, "Dickkopf-1 (DKK-1) stimulated prostate cancer growth and metastasis and inhibited bone formation in osteoblastic bone metastases," *Prostate*, 2011, **71**, 615-625.
24. R. M. Johann, "Cell trapping in microfluidic chips," *Anal. Bioanal. Chem.*, 2006, **385**, 408–412.

25. J. Nilsson, M. Evander, B. Hammarstrom and T. Laurell, “Review of cell and particle trapping in microfluidic systems,” *Analytica Chimica Acta*, 2009, **649**, 141–157.

26. S. Zheng, H. Lin, J.Q. Liu, M. Balic, R. Datar, R.J. Cote and Y.C. Tai, “Membrane microfilter device for selective capture, electrolysis and genomic analysis of human circulating tumor cells,” in: 21st International Symposium on Microscale Bioseparations, *Elsevier Science BV*, Vancouver, Canada, 2007, p. 154.

27. W.H. Tan and S. Takeuchi, “A trap-and-release integrated microfluidic system for dynamic microarray applications,” *Proc. Natl. Acad. Sci. U.S.A.*, 2007, **104**, 1146.

28. D. Di Carlo, N. Aghdam and L.P. Lee, “Single-cell enzyme concentrations, kinetics, and inhibition analysis using high-density hydrodynamic cell isolation arrays,” *Anal. Chem.*, 2006, **78**, 4925.

29. C. Probst, A. Grünberger, W. Wiechert and D. Kohlheyer, “Polydimethylsiloxane (PDMS) sub-micron traps for single-cell analysis of bacteria,” *Micromachines* 2013, **4**, 357-369.

30. D. Wlodkowic, S. Faley, M. Zagnoni, J. P. Wikswo and J. M. Cooper, “Microfluidic single-cell array cytometry for the analysis of tumor apoptosis,” *Anal. Chem.*, 2009, **81**, 5517–5523.

31. J. Kim, J. Erath, A. Rodriguezb and C. Yangac, “A high-efficiency microfluidic device for size-selective trapping and sorting,” *Lab Chip*, 2014, **14**, 2480-2490.

32. X. Xu, P. Sarder, Z. Li and A. Nehora, “Optimization of microfluidic microsphere-trap arrays,” *Biomicrofluidics*, 2013, **7**, 014112.

33. X. Xu, Z. Li, P. Sarder, N. Kotagiri and A. Nehoraia, "Simultaneous detection of multiple biological targets using optimized microfluidic microsphere-trap arrays," *J. Micro/Nanolith. MEMS MOEMS*, 2014, **13(1)**, 013017.

34. X. Xu, Z. Li, N. Kotagiri, P. Sarder, S. Achilefu and A. Nehorai, "Microfluidic microsphere-trap arrays for simultaneous detection of multiple targets," Microfluidics, BioMEMS, and Medical Microsystems XI, *Proc. of SPIE*, 2013, **8615**.

35. C. Jen, J. Hsiao and N. A. Maslov, "Single-cell chemical lysis on microfluidic chips with arrays of microwells," *Sensors*, 2012, **12**, 347-358.

36. J. Y. Park, M. Morgan, A. N. Sachs, J. Samorezov, R. Teller, Y. Shen, K. J. Pienta and S. Takayama, "Single cell trapping in larger microwells capable of supporting cell spreading and proliferation*," Microfluid Nanofluidics*, 2010, **8(2)**, 263–268.

37. W.H. Tan and S. Takeuchi, "Dynamic microarray system with gentle retrieval mechanism for cell-encapsulating hydrogel beads," *Lab Chip*, 2008, **8**, 259.